Soft Matter

PAPER

View Article Online
View Journal | View Issue

Cite this: *Soft Matter*, 2016, 12, 1452

Controlling and predicting droplet size of nanoemulsions: scaling relations with experimental validation†

Ankur Gupta,[a] H. Burak Eral,[b] T. Alan Hatton[a] and Patrick S. Doyle*[a]

Received 17th August 2015,
Accepted 24th November 2015

DOI: 10.1039/c5sm02051d

www.rsc.org/softmatter

Nanoemulsions possess powerful nano-scale properties that make them attractive for diverse applications such as drug delivery, food supplements, nanoparticle synthesis and pharmaceutical formulation. However, there is little knowledge in nanoemulsion literature about controlling and predicting droplet size. In this article, we propose a scaling relation to predict the dependence of nanoemulsion droplet size with physical properties such as viscosity of the droplet phase and continuous phase, and process parameters such as input power density. We validate our proposed scaling with a wide range of droplet size data from nanoemulsions prepared with high pressure homogenization and ultrasonication. Our proposed scaling also compares favorably with experimental data from literature. The scaling relation can serve as a guiding principle for rational design of nanoemulsions.

1 Introduction

Nanoemulsions consist of droplets on the order of 100 nm stabilized by an emulsifier. There are primarily two types of nanoemulsions: oil-in-water (O/W) and water-in-oil (W/O). Due to their exceptional properties such as high surface area per unit volume, long shelf life, transparent appearance and tunable rheology, nanoemulsions have been an active area of research over the past decade or so.[1–4] Nanoemulsions have been used in drug delivery research as a medium to transport hydrophobic drugs dissolved in the oil phase.[5–8] In the food industry, nanoemulsions have been used to develop smart drinks which consist of healthy hydrophobic components like β-carotene and circumin in the oil phase.[9–11] Nanoemulsions have also been explored for other research areas like nanoparticle synthesis[12–14] and pharmaceutical crystallization.[15]

Two widely used high energy methods to prepare nanoemulsions are high pressure homogenization (HPH) and ultrasonication (Fig. 1). In HPH, a mixture of oil, water and surfactant is pushed through a small gap where droplets experience extreme shear and elongational stress.[16] The gap height is typically on the order of 1–10 μm and therefore the pressure drop (ΔP) across HPH can reach a few thousand bars.[16–18] Due to high level of stress inside the homogenizer, droplets deform and break into smaller droplets (Fig. 1(a)). The mixture is typically passed multiple times through the homogenizer until the droplet size is roughly constant[2,17,19] (referred as number of passes, N). In ultrasonication, electrical signals are converted into mechanical vibrations. These mechanical vibrations create sinusoidal pressure variations in the surrounding medium. During one of the low pressure cycles, cavitation results in formation of bubbles. These bubbles contract and expand until implosion, creating disturbance in the local flow field which ultimately breaks the droplet[20–22] (Fig. 1(b)). Like homogenization, ultrasonication is also continued for sufficient time until the droplet size is roughly constant.[19,23] Low energy methods to prepare nanoemulsions like emulsion inversion point,[24] phase inversion temperature[25] and bubble bursting at an oil/water interface[26] have also been developed. However, in this article, we will restrict the discussion to high energy methods.

There is a rich theoretical understanding about the prediction of droplet size of macroemulsions, *i.e.* emulsions with droplet size on the order of 10 μm or larger. The macroemulsion literature mostly uses either Taylor's theory[27] or Hinze's theory[28] to predict the droplet size. Taylor's theory was developed for low Reynolds number (Re) flow with simple flow fields.[27] On the other hand, Hinze's theory was built on the assumption that during emulsification, the flow is completely turbulent.[28] Though these theories represent completely different flow regimes and were developed for macroemulsions, many modern nanoemulsion studies have referred to Taylor's theory as well as Hinze's theory to explain trends observed in droplet size.[2,17,18,20,23,29–37] However, few studies also acknowledge that the agreement with Taylor's and Hinze's theory is only qualitative at best and that these theories should be used only for an order of magnitude estimation of droplet size.[17,23] Further, there are also experimental studies on

[a] *Massachusetts Institute of Technology, Cambridge, MA, USA. E-mail: pdoyle@mit.edu; Fax: +31 617 324 0066; Tel: +31 617 253 4534*
[b] *Delft University of Technology, The Netherlands*

† Electronic supplementary information (ESI) available. See DOI: 10.1039/c5sm02051d

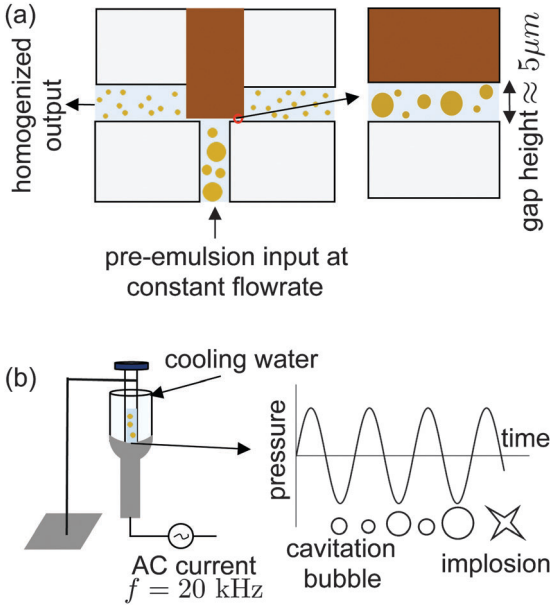

Fig. 1 Schematic of high pressure homogenizer (HPH) and ultrasonicator used for making nanoemulsions. (a) HPH consists of a small gap with height on the order of 5 μm through which the mixture of oil, water and surfactant is pushed. During this process, the droplets experience extreme shear and elongational stress and reduce to a smaller size. Typically, this process is repeated many times and is referred to as number of passes (N). (b) In ultrasonication, electrical signals are converted into mechanical vibrations which create pressure fluctuations in the surrounding medium. Cavitation bubbles form, expand and contract due to these fluctuations until their implosion which creates disturbance in the surroundings leading to local turbulence and breakup of large droplets into smaller ones.

nanoemulsion which do not use any theoretical prediction and fit their droplet size data using empirical power law correlations.[19,37–40] For instance, experimental studies have shown that nanoemulsion size increases with increase in droplet viscosity (μ_d) and decreases with increase in continuous phase viscosity (μ_c).[29,37,40] Hence, this article focuses on bridging the gap between experimental observations and theoretical predictions for nanoemulsion droplet size.

In this article, we first review the theories proposed by Taylor[27] and Hinze[28] and argue that the correlations developed for macroemulsions cannot be directly used for nanoemulsions. We then modify Hinze's theory[28] based on more appropriate hydrodynamic light scales to accurately predict the droplet size of nanoemulsions. We also validate our proposed scaling by generating a wide range of experimental data, as well as comparing to existing data from literature. The new scaling relation is able to quantitatively predict droplet size variation with physical properties and hence enables rationale design of nanoemulsions prepared by high energy methods.

2 Theory

We review the classical work of Taylor[27] that describes the relationship between the fluid flow and the droplet size of macroemulsions. Taylor performed experimental and theoretical analysis on a single droplet being deformed by laminar flow field. Taylor suggested that a droplet will not break unless the applied stress ($\tau_{applied}$) deforming the droplet exceeds the interfacial stress $\left(\frac{\sigma}{d}\right)$ holding the droplet in the same shape. Hence, Taylor defined a critical capillary number, $Ca_{crit,d} \sim \frac{\tau_{applied} d}{\sigma}$ below which the droplet will not break. Mathematically, Taylor's criteria for droplet breakup can be expressed as:

$$Ca_{crit,d} = C_1 \quad (1)$$

where C_1 is a constant. The applied stress in a low Re flow is defined as $\tau_{applied} \sim \mu_c \dot{\gamma}$, where, μ_c is the continuous phase viscosity, $\dot{\gamma}$ is the shear rate in the continuous phase. Hence, the droplet size can be defined as:

$$d = C_1 \frac{\sigma}{\mu_c \dot{\gamma}} \quad (2)$$

Taylor (and others) followed up this work and showed that C_1 is a function of $\frac{\mu_d}{\mu_c}$.[41,42] However, nanoemulsion literature has referred to Taylor's theory in the form of eqn (2) and hence, we will use the same form.[2,17,18,20,23]

While Taylor's theory provides a very intuitive understanding of droplet deformation, it is not applicable to the turbulent flow produced inside a homogenizer and ultrasonicator used in industrial applications.[43] The most widely used theory for predicting droplet size in industrially prepared macroemulsions was developed by Hinze.[28] Hinze suggested that if a droplet of viscosity μ_d, density ρ_d, interfacial tension with outer phase σ, is deformed by the outer phase with a stress $\tau_{applied}$ (Fig. 2(a)), two dimensionless numbers that govern the problem are the critical Weber number:

$$We_{crit,d} = \frac{\tau_{applied} d}{\sigma} \quad (3)$$

and the Ohnesorge number:

$$Oh = \frac{\mu_d}{\sqrt{\rho_d \sigma d}}. \quad (4)$$

Oh physically represents the ratio of viscocapillary time scale to Rayleigh breakup time scale. Hinze further argued that a critical Weber number below which a droplet will not break is given by:

$$We_{crit,d} = C_2(1 + f(Oh)) \quad (5)$$

where C_2 is a constant (similar to Taylor's approach) and $f(Oh)$ denotes the contribution of viscosity effects of the droplet. Hinze[28] argued that for macroemulsions, since diameter of the droplet is large, $Oh \ll 1$, $f(Oh)$ vanishes and $We_{crit,d} = C_2$. Hinze equated $\tau_{applied}$ to the inertial stress in the continuous phase $\rho_c u_c^2$. This can be re-written as $\rho_c(\varepsilon d)^{2/3}$ according to the classical turbulence theory, where ρ_c, u_c are the density and the velocity scale of the continuous phase respectively, and ε is the power density input. Hence, Hinze derived the widely used result:

$$d = C_2 \left(\frac{\sigma}{\rho_c}\right)^{3/5} \varepsilon^{-2/5} \quad (6)$$

Since nanoemulsions are typically prepared through a homogenizer or an ultrasonicator (where the flow is turbulent),

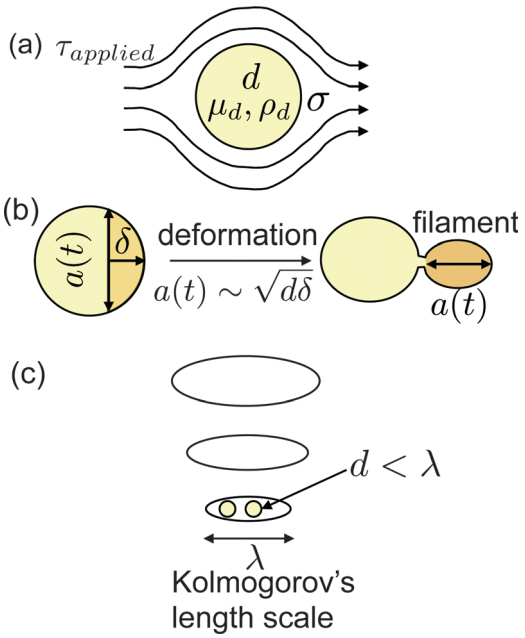

Fig. 2 Schematic of the proposed mechanism for nanoemulsion formation. (a) Consider a droplet with diameter d, viscosity μ_d, density ρ_d, interfacial tension with surrounding medium σ being deformed by an applied stress $\tau_{applied}$. (b) Physically, a droplet will break when a filament coming out of the parent droplet has sufficient inertial stress to overcome the interfacial stress. Assuming an instability propagation of length scale δ, the length scale of filament can be estimated as $a(t) \sim \sqrt{d\delta}$. (c) The nanoemulsion droplets are so small that they are typically smaller than the smallest eddy created by the turbulent flow. The size of smallest eddy is determined by the Kolomogorov's length scale (λ). Hence, $\tau_{applied}$ scales as the stress inside the smallest eddy.

we decided to build upon the work of Hinze. If we assume typical values for nanoemulsions of $d \approx 100$ nm, $\mu_d \approx 10$ cP, $\rho_d \approx 1000$ kg m^{-3}, $\sigma \approx 10$ mN m^{-1}, we calculate that Oh ≈ 10. Therefore, one cannot assume $f(\mathrm{Oh}) \approx 0$ and we need to define a new criteria of critical Weber number for the large Oh regime.

An overview of the proposed mechanism for nanoemulsion formation is provided in Fig. 2. We propose that prior to droplet breakup, a filament extrudes out from the parent droplet due to an instability at the surface. Similar to literature on the impact of droplet on a solid surface, we propose that for a droplet to break, the inertial stress of the filament extruding from the parent droplet has to exceed the interfacial stress.[44,45] Let us assume that an instability of length $\delta \sim u_d t$ has penetrated inside the parent droplet, where u_d is the velocity scale inside the droplet given by Hinze[28] as $\sqrt{\frac{\tau_{applied}}{\rho_d}}$ and t is the propagation time of the instability (Fig. 2(b)). Conservation of mass dictates that volume of the filament and the hypothetical cap formed by the instability are equal. Upon geometrical calculations, we find that the diameter of the base of the spherical cap scales as $a(t) \sim 2\sqrt{\frac{d^2}{4} - \left(\frac{d}{2} - \delta\right)^2} \sim \sqrt{d\delta}$. Hence, the volume of this spherical cap scales as $V_{s,cap} \sim a(t)^2\delta \sim d\delta^2$. We can also define the velocity scale inside the filament as $u_a \sim \frac{d}{dt}(a(t)) \sim u_d\sqrt{\frac{d}{\delta}}$.

Now, we will do a general derivation to define the criteria for droplet breakup. This derivation reduces to Hinze's result for low values of Ohnesorge number. However, for large Ohnesorge number (a regime relevant to nanoemulsions), we obtain a completely different result. To arrive at a droplet breakup criteria, we need to evaluate the filament properties when the droplet breaks. For the regime of Oh $\ll 1$, since the viscous effects inside the droplet are negligible, the droplet breakup time scale ($t \sim t_{breakup}$) is dominated by the convective time scale. In other words, the droplet break up time scale is simply given by $t_{breakup} \sim \frac{d}{u_d}$. Hence, for the Oh $\ll 1$, at $t \sim t_{breakup}$ one has $\delta \sim a \sim d$ and $u_a \sim u_d$. On the other hand, for Oh > 1, the viscous stresses inside the drop would start to play an important role and hence the droplet breakup time scale would be dominated by the diffusive time scale $t_{breakup} \sim \frac{\mu_d}{u_d{}^2\rho_d}$. In this regime, we can also think of droplet breakup time scale as $t_{breakup} \sim \frac{d}{u_d}\mathrm{Re}_d{}^{-1}$, where Re_d is the droplet Reynolds number given as $\mathrm{Re}_d \sim \frac{\rho_d u_d d}{\mu_d} \sim \frac{\sqrt{\mathrm{We}_{crit,d}}}{\mathrm{Oh}}$. Therefore, for Oh > 1, at $t \sim t_{breakup}$, $\delta \sim d\mathrm{Re}_d{}^{-1}$, $a \sim d\mathrm{Re}_d{}^{-0.5}$ and $u_a \sim u_d\mathrm{Re}_d{}^{0.5}$. We observe that in large Oh regime, since the viscous stresses inside the droplet are important, a and u_a are strongly dependent on Re_d. Now, we can mathematically define the breakup criteria of the filament:

$$\mathrm{We}_{crit,a} = \left(\frac{\rho_d u_a{}^2 a}{\sigma}\right)\Big|_{t=t_{breakup}} = C_3 \qquad (7)$$

where C_3 is a constant. Since, for Oh $\ll 1$, $\delta \sim a \sim d$, $u_a \sim u_d$, eqn (7) can be re-written as:

$$\mathrm{We}_{crit,a} = \frac{\rho_d u_d{}^2 d}{\sigma} = \frac{\tau_{applied} d}{\sigma} = \mathrm{We}_{crit,d} = C_3 \qquad (8)$$

which is exactly the same as what Hinze predicted for low Oh. On the other hand, for large Oh, since, $\delta \sim d\mathrm{Re}_d{}^{-1}$, $a \sim d\mathrm{Re}_d{}^{-0.5}$ and $u_a \sim u_d\mathrm{Re}_d{}^{0.5}$, eqn (7) can be re-written:

$$\mathrm{We}_{crit,a} = \frac{\rho_d u_d{}^2 d}{\sigma}\mathrm{Re}_d{}^{0.5} = \mathrm{We}_{crit,d}\mathrm{Re}_d{}^{0.5} = C_3 \qquad (9)$$

Substituting Re_d in terms of Oh and $\mathrm{We}_{crit,d}$, we get:

$$\mathrm{We}_{crit,d} = C_4\mathrm{Oh}^{2/5} \qquad (10)$$

Eqn (10) shows the variation of $\mathrm{We}_{crit,d}$ with Oh for the large Oh regime. For a large value of Oh, due to the increasing importance of the viscous stresses inside the droplet, higher inertial stress (or $\mathrm{We}_{crit,d}$) is required for the filament to break away from the droplet. However, to define $\mathrm{We}_{crit,d}$, we also need to define $\tau_{applied}$.

$\tau_{applied}$ is governed by the flow dynamics of the continuous phase around the droplet. Although flow in a homogenizer and ultrasonicator is turbulent in bulk (see ESI† for more details), the flow around droplets is still viscous. This can be seen by the relative values of the smallest eddy size (or the Kolmogorov's length scale), λ and the droplet size, d (Fig. 2(c)). The value of λ

is given by $\left(\frac{{\mu_c}^3}{\varepsilon{\rho_c}^3}\right)^{1/4}$.[46,47] Assuming the value of $\mu_c \approx 1$ cP, $\rho_c \approx 1000$ kg m^{-3} and $\varepsilon \approx 10^8$ W kg^{-1},[43] we get, $\lambda \approx 300$ nm. Since, $d \approx 100$ nm, nanoemulsions are on the similar length scale as the smallest eddy and hence, the flow around them is viscous. Therefore, $\tau_{applied}$ should be given by the stress inside the smallest eddy, or, $\tau_{applied} \sim \sqrt{\mu_c \rho_c \bar{\varepsilon}}$. This regime is called the viscous turbulent regime and has been recently validated experimentally.[46,47] This has also been recognized by Nazarzadeh *et al.* where authors mentioned nanoemulsion droplets are smaller than the smallest eddy.[36] However, they did not recognize that nanoemulsions lie in the large Oh regime. Hence, using $\tau_{applied} \sim \sqrt{\mu_c \rho_c \bar{\varepsilon}}$ in eqn (3) and (10), we get:

$$d = C_3 \frac{\sigma^{5/6} {\mu_d}^{1/3}}{(\rho_d \sigma)^{1/5} (\mu_c \rho_c \varepsilon)^{5/12}} \quad (11)$$

Eqn (11) is valid for the viscous turbulent regime (turbulent flow in bulk and viscous flow around the droplets) with large Oh. Eqn (11) predicts the following trends for nanoemulsion droplet size:

$$d \sim {\mu_d}^{1/3} \quad (12)$$

$$d \sim {\mu_c}^{-5/12} \quad (13)$$

$$d \sim \varepsilon^{-5/12} \quad (14)$$

The above equations can serve as a design principle for controlling and predicting the droplet size of nanoemulsions. The current prediction is able to capture the effect of both μ_c and μ_d, unlike the correlations proposed by Hinze.[28] Additionally, our prediction of $d \sim \varepsilon^{-5/12}$ is very similar to Hinze's prediction of $d \sim \varepsilon^{-2/5}$.

3 Results and discussion

We prepared O/W nanoemulsions using both high pressure homogenizer (HPH) and ultrasonication. We systematically varied the oil phase viscosity to encompass a wide range of Oh. We prepared nanoemulsions with the following composition: 1% (v/v) oil–175 mM sodium dodecyl sulphate (SDS)–water. The values of physical properties of the oil phase are summarized in Table 1 (details in ESI†). The interfacial tension given here is measured in the presence of surfactant well above its critical micelle concentration. We chose SDS as the surfactant in order to avoid emulsifier-size effects.[29,40] In HPH experiments, we homogenized each nanoemulsion system for 4 different pressure drops with 20 passes each. In ultrasonication experiments, we sonicated each nanoemulsion system at 3 different sonication amplitudes for 20 minutes each. The size and polydispersity was measured using dynamic light scattering (DLS). The details of size and polydispersity calculations from raw DLS data are provided in ESI.†

Fig. 3(a) shows the droplet size variation for silicone oil nanoemulsions obtained from HPH. As expected, the droplet size decreases with pressure drop (ΔP) and number of passes (N). This is consistent with the observations from the literature.[2,18,19]

Table 1 Physical properties of oil phases used to prepare nanoemulsions

Oil	μ_d (cP)	ρ_d (kg m^{-3})	σ (mN m^{-1})
Hexadecane	3	764	4.9
Silicone oil	4	914	7.6
75–25 silicone mixture	12	916	8.8
50–50 silicone mixture	22	928	9.0
Mineral	24	840	7.4
25–75 silicon mixture	46	938	7.9
Viscous silicone oil	97	958	8.7

Also, the droplet size follows an exponentially decaying function with N (shown by solid lines in Fig. 3(a)). This is a classic signature of a system that has no coalescence and is dominated by droplet breakage. Polydispersity remains practically constant ($\approx$25%) suggesting that the average size of the droplet is a good representative of the distribution. Since we are in interested in validating $We_{crit,d}$, we assume that the diameter after 20 passes (d_{20}) will not change significantly on further emulsification. The variations of d_{20} with ΔP for all the nanoemulsion systems prepared using HPH are shown in Fig. 3(b). Experimental results clearly show that d_{20} is dependent of μ_d as well as ΔP. As μ_d increases, droplet size increases and as ΔP increases, droplet size decreases.

The results for droplet size variations for silicone oil nanoemulsions obtained from ultrasonication are shown in Fig. 3(c and d). Similar to the dependence of droplet size with number of passes in HPH, the droplet size variation with ultrasonication time decays exponentially. The variation of d_{20} (size after 20 minutes of sonication) for all the nanoemulsion systems prepared using ultrasonicator are shown in Fig. 3(d). One immediately observes while comparing Fig. 3(b) and (d) that the size range of nanoemulsions obtained from the homogenizer and ultrasonicator is almost identical. Also, the effect of μ_d on d_{20} follows the same trend for both HPH and ultrasonication. However, unlike the effect of ΔP on d_{20} in HPH, change in ultrasonication amplitude does not change d_{20} significantly. This effect has also been observed in literature.[19,23] We explain the reason behind this observation later.

For converting the raw data to $We_{crit,d}$, we estimated the value of ε for both the homogenizer (ε_h) and ultrasonicator (ε_s). We estimate that $\varepsilon_h \approx \frac{Q\Delta P}{V_{homogenizer}\rho_c}$ where Q is the flowrate and $V_{homogenizer}$ is the volume of the homogenizer.[37,48] For the homogenizer used in our experiments, $Q \approx 10^{-6}$ m^3 s^{-1}, $\Delta P \approx 10^8$ Pa, $\rho_c \approx 10^3$ kg m^{-3}, $V_{homogenizer} \approx 10^{-9}$ m^3 and hence, $\varepsilon_h \approx 10^8$ W kg^{-1}. Since Q is constant for our homogenizer, $\varepsilon_h \sim \Delta P$ (please see ESI† for more details). ε_s was estimated using the correlation, $\varepsilon_s \approx \frac{P_b + P_{atm}}{\tau_b \rho_c}$, where P_b is the average cavitation collapse pressure, P_{atm} is the atmospheric pressure, τ_b is the bubble collapse time scale.[22] Using the correlations mentioned in the literature,[22] $P_b \approx 10^5$ Pa, $\tau_b \approx 1$ μs, $\rho_c \approx 1000$ kg m^{-3} and hence, $\varepsilon_s \approx 10^8$ W kg^{-1}. The dependence of ε_s is non-monotonic since an increase in the amplitude increases both P_b and τ_b (please see ESI† for more details). Some observations can be made from the estimated

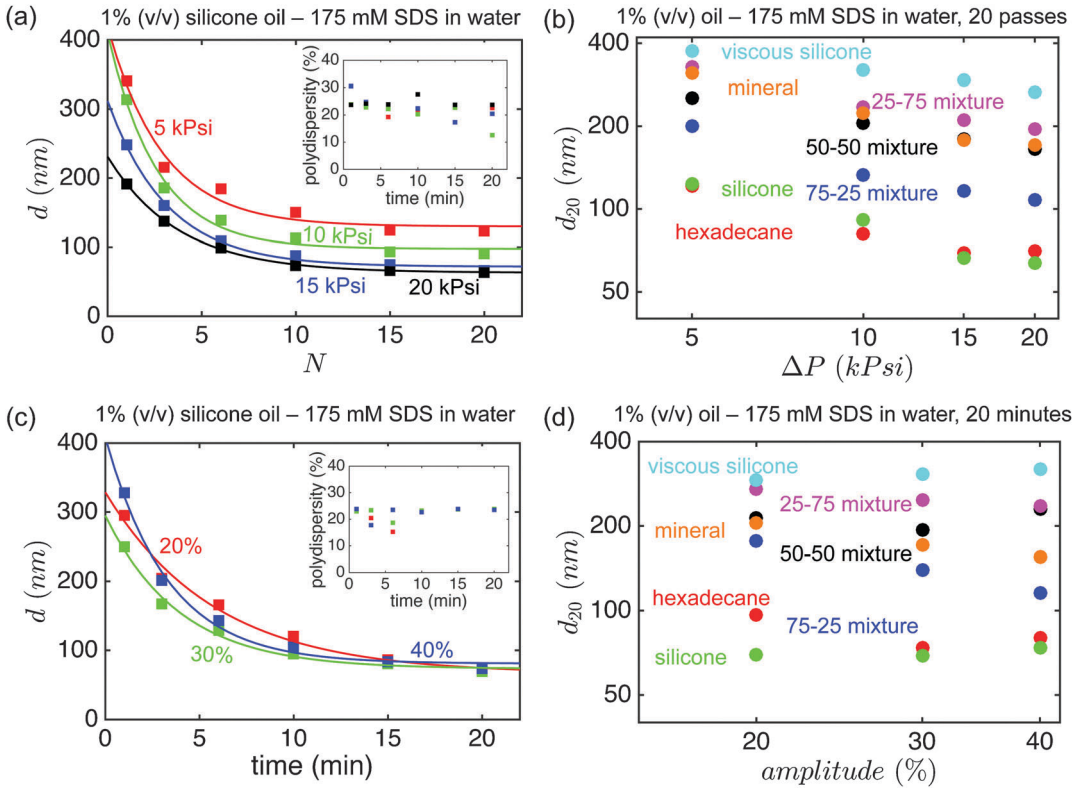

Fig. 3 Summary of nanoemulsion droplet size obtained from experiments. (a) Average droplet size and polydispersity variation for silicone oil nanoemulsions prepared by homogenization at different pressure drops (ΔP) and number of passes (N). The size variation can be fitted with a decaying exponential function which is a classic signature of a system which is dominated by droplet breakage. (b) The diameter after 20 passes (d_{20}) for different oils and ΔP. A clear dependence of d_{20} with μ_d and ΔP is observed. (c) Average droplet size and polydispersity variation for silicone oil nanoemulsions prepared by ultrasonication for different amplitudes and ultrasonication time. The size decreases with ultrasonication time but is insensitive to ultrasonication amplitude. (d) d_{20} show a clear dependence on μ_d.

values of ε_h and ε_s. First, both ε_h and ε_s are on similar order of magnitude which corroborates the observation that size range from nanoemulsion for both HPH and ultrasonication is similar (Fig. 3(b and d)). The variation of $\varepsilon_h \sim \Delta P$ supports the observation that size decreases as ΔP increases (Fig. 3(b), eqn (14)). Similarly, since ε_s is insensitive to change in ultrasonication amplitude, the droplet size does not show a significant variation with amplitude (Fig. 3(d), eqn (14)). Finally, since ε_h and ε_s are on the order of 10^8 W kg^{-1}, we can assume that nanoemulsion formation takes place in the viscous turbulent regime.

We fitted the $We_{crit,d}$ *vs.* Oh data (Fig. 4) with a two parameter power law model and the fits to the experimental data yield scalings very close to the proposed scaling of $We_{crit,d} \sim Oh^{2/5}$. There are some conclusions one can draw from Fig. 4.

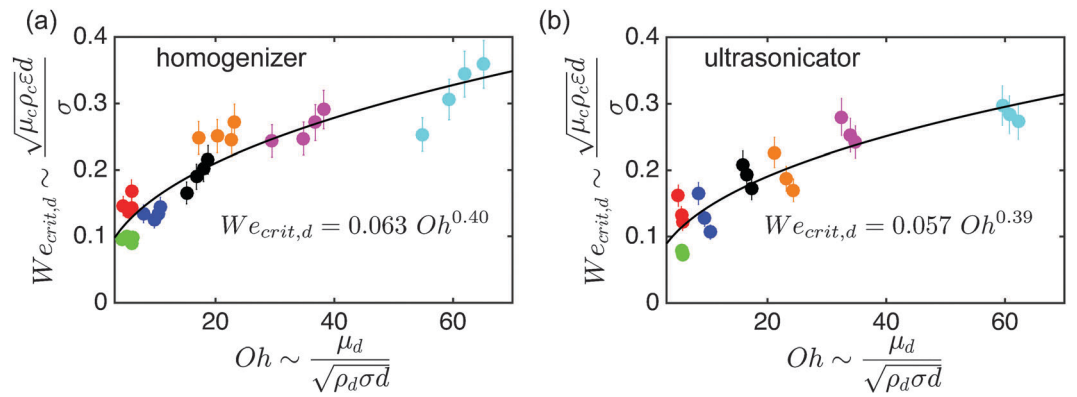

Fig. 4 Experimental validation of the proposed scaling relation $We_{crit,d} \sim Oh^{0.4}$. A two parameter fit predicts a power law exponent very close to the proposed scaling relation and with similar prefactors for both the homogenizer and ultrasonicator data. The different colors represent different oil phases.

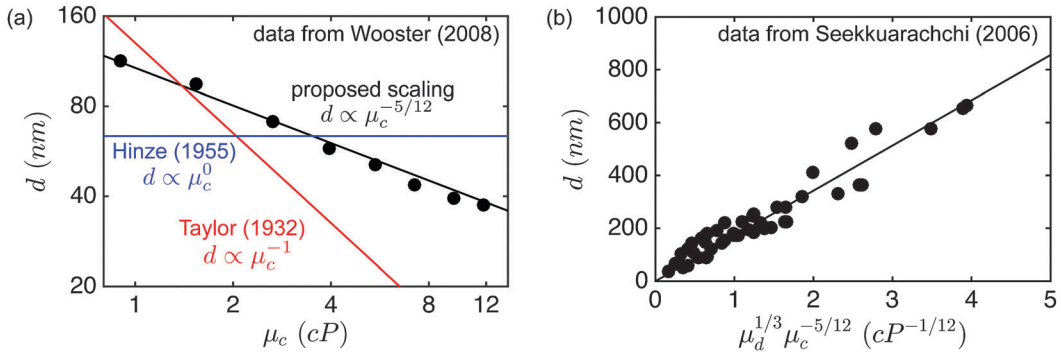

Fig. 5 Validation of proposed scaling with experimental data from literature. (a) The data has been taken from Wooster *et al.*[29] where the authors increased the continuous phase viscosity. As shown, our proposed scaling of $d \propto \mu_c{}^{-5/12}$ agrees well with the experimental data. On the other hand, modern nanoemulsion studies[2,17,18,20,23,29–37] have incorrectly extrapolated the theories of Taylor[27] and Hinze[28] to predict nanoemulsion droplet size. (b) The data has been taken from Seekkuarachchi *et al.*[37] where the authors varied both dispersed phase viscosity as well as continuous phase viscosity. Our proposed scaling is in good agreement with the experimental data.

First, we observe that nanoemulsion synthesis indeed lies in the large Oh regime. Also, we can clearly see that the proposed scaling is able to capture the variation of μ_d for both homogenizer and ultrasonicator data. Interestingly, the similarity in predicted exponents and pre-exponential factor for both the homogenizer and ultrasonicator suggests a universal collapse of data for nanoemulsions prepared through different two different methods (see ESI†). This shows the merit of approaching droplet size prediction using dimensionless analysis. However, there is some scatter in the data around the predicted values within the same oil phase. We believe that this scatter is due to error present in the estimation of ε_h and ε_s. Since homogenization and ultrasonication involve complex and dynamic processes, there is high uncertainty in the estimation of power density.

To validate the predicted trend of droplet size on μ_c, we replotted the experimental data from Wooster *et al.*[29] (Fig. 5(a)) where researchers added PEG to water phase for O/W nanoemulsions to vary μ_c. As noted previously, we predict a scaling of $d \sim \mu_c{}^{-5/12}$ as mentioned in eqn (13). Taylor's theory predicts a scaling of $d \sim \mu_c{}^{-1}$ (eqn (2)) whereas Hinze's theory predicts a scaling of $d \sim \mu_c^0$ (eqn (6)). There is excellent agreement between experimental data predicted with our proposed scaling. However, Taylor's theory over predicts the variation of droplet size of μ_c whereas Hinze's theory under predicts the variation of droplet size with μ_c. Modern nanoemulsion literature has incorrectly extrapolated Taylor's and Hinze's theory[2,17,18,20,23,29–37] to explain the trends in nanoemulsion droplet size.

We also validated our scaling relation with the data from Seekkuarachchi *et al.*[37] We re-plotted the size data for nanoemulsion systems prepared at the same homogenization condition but with wide range of μ_d and μ_c. Since the variations in ρ_d and σ were negligible across different formulations, we plotted the variation of d with our predicted scaling in Fig. 5(b) (eqn (12) and (13)). We obtain excellent agreement from our scaling relation with an extensive set of experimental data.

To conclude, in this article, we proposed a scaling relation to predict nanoemulsion droplet size based on the fundamentals of filament breakup. Our proposed scaling, $We_{crit,d} = C_4 Oh^{2/5}$, is able to quantitatively predict the droplet size of nanoemulsions. The strongest aspect of our proposed scaling is its ability to predict the trends in droplet size with droplet viscosity as well as continuous phase viscosity. Our scaling relation fits a large range of experimental data obtained for completely different nanoemulsion systems and prepared through different techniques. Also, the dimensionless form of scaling can be used as a guiding principle to identify critical parameters and enable rational design of nanoemulsions.

4 Material and methods

Materials

Hexadecane, silicone oil (5 cSt, 100 cSt), mineral oil and SDS are products from Sigma Aldrich.

Methods

Pre-emulsion for HPH and ultrasonication was prepared by mixing 175 mM SDS aqueous solution with 1% (v/v) oil phase using a magnetic stirrer bar for 30 minutes at 700 rpm. 30 mL of pre-emulsion was homogenized in Avestin C-3 homogenizer with four different pressure drops (5, 10, 15, 20 kPsi) and 20 passes each. 2 mL pre-emulsion was ultrsonicated at three different amplitudes (20, 30, 40%) in an ultrasonicator with a 24 mm horn diameter (from Cole Parmer) at a frequency of 20 kHz. The prepared nanoemulsion was diluted 10 times in DI water and then used as a sample for dynamic light scattering (DLS). 3 independent measurements were taken for each sample. Each DLS measurement involved 10 acquisitions of 5 seconds each. Size and polydispersity were extracted from raw DLS data using second order cumulant analysis (details in the ESI†).

Acknowledgements

The authors would like to thank Eni SPA for providing funds for this project. We acknowledge The Biophysical Instrumentation Facility at MIT for providing us with the DLS support (NSF-0070319). We also acknowledge the contribution of Bavand Keshavarz for helping us out with the theoretical understanding of droplet splash.

References

1 A. Gupta, H. E. Burak, T. A. Hatton and P. S. Doyle, *Soft Matter*, 2015, under review.
2 T. G. Mason, S. M. Graves, J. N. Wilking and M. Y. Lin, *Condens. Matter Phys.*, 2006, **9**, 193–199.
3 T. Tadros, P. Izquierdo, J. Esquena and C. Solans, *Adv. Colloid Interface Sci.*, 2004, **108–109**, 303–318.
4 C. Solans, P. Izquierdo, J. Nolla, N. Azemar and M. Garciacelma, *Curr. Opin. Colloid Interface Sci.*, 2005, **10**, 102–110.
5 M. Kumar, A. Misra, A. K. Babbar, A. K. Mishra, P. Mishra and K. Pathak, *Int. J. Pharm.*, 2008, **358**, 285–291.
6 D. Sarker, *Curr. Drug Delivery*, 2005, **2**, 297–310.
7 C. Lovelyn, *J. Biomater. Nanobiotechnol.*, 2011, **02**, 626–639.
8 F. Shakeel, S. Baboota, A. Ahuja, J. Ali, M. Aqil and S. Shafiq, *AAPS PharmSciTech*, 2007, **8**, E104.
9 D. J. McClements and J. Rao, *Crit. Rev. Food Sci. Nutr.*, 2011, **51**, 285–330.
10 D. J. McClements, *Soft Matter*, 2011, **7**, 2297–2316.
11 J. Rao and D. J. McClements, *Food Hydrocolloids*, 2011, **25**, 1413–1423.
12 N. Anton, J.-P. Benoit and P. Saulnier, *J. Controlled Release*, 2008, **128**, 185–199.
13 K. Landfester, *Angew. Chem., Int. Ed.*, 2009, **48**, 4488–4507.
14 J. M. Asua, *Prog. Polym. Sci.*, 2002, **27**, 1283–1346.
15 H. B. Eral, V. López-Mejías, M. O'Mahony, B. L. Trout, A. S. Myerson and P. S. Doyle, *Cryst. Growth Des.*, 2014, **14**, 2073–2082.
16 J. Floury, J. Bellettre, J. Legrand and A. Desrumaux, *Chem. Eng. Sci.*, 2004, **59**, 843–853.
17 T. G. Mason, J. N. Wilking, K. Meleson, C. B. Chang and S. M. Graves, *J. Phys.: Condens. Matter*, 2006, **18**, R635–R666.
18 M. E. Helgeson, S. E. Moran, H. Z. An and P. S. Doyle, *Nat. Mater.*, 2012, **11**, 344–352.
19 S. Y. Tang, P. Shridharan and M. Sivakumar, *Ultrason. Sonochem.*, 2013, **20**, 485–497.
20 T. S. H. Leong, T. J. Wooster, S. E. Kentish and M. Ashokkumar, *Ultrason. Sonochem.*, 2009, **16**, 721–727.
21 S. Abbas, K. Hayat, E. Karangwa, M. Bashari and X. Zhang, *Food Eng. Rev.*, 2013, **5**, 139–157.
22 T. J. Mason and J. P. Lorimer, *Applied Sonochemistry*, Wiley-VCH, 2002.
23 T. Delmas, H. Piraux, A.-C. Couffin, I. Texier, F. Vinet, P. Poulin, M. E. Cates and J. Bibette, *Langmuir*, 2011, **27**, 1683–1692.
24 A. Forgiarini, J. Esquena, C. Gonzalez and C. Solans, *Langmuir*, 2001, **17**, 2076–2083.
25 P. Izquierdo, J. Esquena, T. F. Tadros, C. Dederen, M. Garcia, N. Azemar and C. Solans, *Langmuir*, 2002, **18**, 26–30.
26 J. Feng, M. Roché, D. Vigolo, L. N. Arnaudov, S. D. Stoyanov, T. D. Gurkov, G. G. Tsutsumanova and H. A. Stone, *Nat. Phys.*, 2014, **10**, 606–612.
27 G. I. Taylor, *Proc. R. Soc. London, Ser. A*, 1932, **138**, 41–48.
28 J. O. Hinze, *AIChE J.*, 1955, **1**, 289–295.
29 T. J. Wooster, M. Golding and P. Sanguansri, *Langmuir*, 2008, **24**, 12758–12765.
30 K. Meleson, S. Graves and T. G. Mason, *Soft Mater.*, 2004, **2**, 109–123.
31 V. Ghosh, A. Mukherjee and N. Chandrasekaran, *Ultrason. Sonochem.*, 2013, **20**, 338–344.
32 S. Kotta, A. W. Khan, K. Pramod, S. H. Ansari, R. K. Sharma and J. Ali, *Expert Opin. Drug Delivery*, 2012, **9**, 585–598.
33 Z. Han, B. Yang, Y. Qi and J. Cumings, *Ultrasonics*, 2011, **51**, 485–488.
34 S. M. Graves and T. G. Mason, *J. Phys. Chem. C*, 2008, **112**, 12669–12676.
35 J. Schmidt, C. Damm, S. Romeis and W. Peukert, *Chem. Eng. Sci.*, 2013, **102**, 300–308.
36 E. Nazarzadeh and S. Sajjadi, *AIChE J.*, 2010, **56**, 2751–2755.
37 I. N. Seekkuarachchi, K. Tanaka and H. Kumazawa, *Ind. Eng. Chem. Res.*, 2006, **45**, 372–390.
38 F. Dons, M. Sessa and G. Ferrari, *Ind. Eng. Chem. Res.*, 2012, **51**, 7606–7618.
39 T. Gothsch, J. H. Finke, S. Beinert, C. Lesche, J. Schur, S. Büttgenbach, C. Müller-Goymann and a. Kwade, *Chem. Eng. Technol.*, 2011, **34**, 335–343.
40 C. Qian and D. J. McClements, *Food Hydrocolloids*, 2011, **25**, 1000–1008.
41 G. Taylor, *Proc. R. Soc. London, Ser. A*, 1934, 501–523.
42 B. J. Bentley and L. G. Leal, *J. Fluid Mech.*, 1986, **167**, 241.
43 J. Davies, *Chem. Eng. Sci.*, 1987, **42**, 1671–1676.
44 J. C. Bird, S. S. H. Tsai and H. A. Stone, *New J. Phys.*, 2009, **11**, 063017.
45 C. Josserand and S. Zaleski, *Phys. Fluids*, 2003, **15**, 1650.
46 R. Shinnar, *J. Fluid Mech.*, 1961, **10**, 259–275.
47 J. A. Boxall, C. A. Koh, E. D. Sloan, A. K. Sum and D. T. Wu, *Langmuir*, 2012, **28**, 104–110.
48 F. Innings and C. Trägårdh, *Exp. Therm. Fluid Sci.*, 2007, **32**, 345–354.

